RevMexAA (Serie de Conferencias), **15**, 317–322 (2003)

SUPERNOVA REMNANT EVOLUTION IN AN AGN ENVIRONMENT

J. M. Pittard,[1] J. E. Dyson,[1] S. A. E. G. Falle,[2] and T. W. Hartquist[1]

RESUMEN

Un aspecto de la evolución de los remanentes de supernova que es poco estudiado es la influencia de un ambiente como el que se encuentra en un núcleo activo galáctico (NAG). Un medio ambiente con densidad alta junto con una fuente de continuo poderosa pueden ayudar al enfriamiento del gas eyectado chocado y del gas barrido, y presentamos resultados recientes de simulaciones numéricas con términos fuentes de calentamiento y enfriamiento apropiados en la ecuación de energía. Uno de nuestros resultados principales es que gas eyectado chocado se enfría rápidamente para asi formar nubes densas y frías con una densidad, un parámetro de ionización, y una densidad columnar compatibles con los valores inferidos para el componente de alta ionización de las regiones de emisión de líneas anchas en los objetos cuasi-estelares (QSOs).

ABSTRACT

One aspect of supernova remnant evolution that is relatively unstudied is the influence of an AGN environment. A high-density ambient medium and a nearby powerful continuum source will assist the cooling of shocked ejecta and swept-up gas, and recent results of simulations with appropriate heating and cooling terms are presented. A central finding is that the shocked ejecta rapidly cool to form cold dense clouds with a density, an ionization parameter, and a column density compatible with those inferred for the high-ionization component of the broad-emission-line regions in QSOs.

Key Words: **GALAXIES: ACTIVE — HYDRODYNAMICS — SHOCK WAVES — SUPERNOVA REMNANTS**

1. INTRODUCTION

Emission lines consistently attract attention in AGN studies because they serve as diagnostics of physical conditions. Over the years we have learnt a great deal about the properties of the gas comprising the broad-emission-line region (BELR). It is photoionized—reverberation studies (e.g., Clavel et al. 1991) show a direct response of emission-line strengths to continuum variability. The absence of deep Lyα absorption indicates that the BELR covers only 5 to 25% of the continuum source (e.g., Bottorff et al. 1997). It has a small volume filling factor ($\sim 10^{-7}$), as determined from the observed line-strength-to-continuum ratio (Blandford et al. 1990). It is also able to generate a wide range of line profile shapes (indicating that the geometry and kinematics is complex and varied), and shows evidence of a two-component structure (Collin-Souffrin, Dumont, & Tully 1982; Cullin-Souffrin et al. 1986; Wills, Netzer, & Wills 1985). One of these components can be identified as consisting of high-ionization lines, including C III], C IV, and other multiply ionized species, and is known as the HIL. The second component can be identified with the low-ionization lines, which include the bulk of the Balmer lines, and lines of singly ionized species (e.g., Mg II, C II, Fe II) and is known as the LIL.

The regions emitting the LIL and HIL display different kinematics, as deduced from studies of the profiles and line widths (e.g., Gaskell 1988; Sulentic et al. 1995), and the HIL are systematically blue-shifted with respect to the LIL (see Sulentic, Marziani, & Dultzin-Hacyan 2000). To account for the variability of the low-ionization Mg II and Balmer lines (e.g., Ferland et al. 1992), the LILs must be optically thick. On the other hand, optically thin gas may account for the Baldwin effect (a negative correlation between the ultraviolet emission-line equivalent width and continuum luminosity, although it remains to be seen if this is due to sample biases cf. Sulentic et al. 2000), and for the Wamsteker-Colina effect (a negative correlation between between the C IV $\lambda\,1549$/Lyα ratio and continuum luminosity, Shields, Ferland, & Peterson 1995).

It is now fairly clear that the Balmer lines form at the surface of an accretion disk, or close to the surface in an accretion-disk wind (e.g., Collin-Souffrin et al. 1988; Marziani et al. 1996). The geometrical distribution and kinematics of the HIL gas is, however, much less clear: it may arise in a spherical outflow, while a biconical "jet-like" distribution is another possibility. Approximately 75% of the total luminosity of the broad-line emission is estimated to arise in the LILs (Collin-Souffrin et al. 1988).

Many theoretical explanations have been proposed for the origin of the BELR. They include:

[1]Department of Physics & Astronomy, [2]Department of Applied Mathematics, The University of Leeds, Leeds, UK.

(i) magnetic acceleration of clouds off accretion discs (Emmering, Blandford, & Shlosman 1992), (ii) the interaction of an outflowing wind with the surface of an accretion disc (Cassidy & Raine 1996), (iii) interaction of stars with accretion discs (Zurek, Siemiginowska, & Colgate 1994), (iv) tidal disruption of stars in the gravitational field of the BH (Roos 1992), (v) interaction of an AGN wind with supernovae and star clusters (Perry & Dyson 1985; Williams & Perry 1994), and (vi) emission from accretion shocks (Fromerth & Melia 2001). Many other models have been identified as containing serious difficulties (see references in Pittard et al. 2001): in particular, any model must survive the "confinement problem", and/or continually generate clouds.

Each of these mechanisms will probably contribute some of the observed BELR gas. However, it is clear that some of the proposed models will be more dominant than others, at least under certain conditions (e.g., the rate of tidally disrupted stars in high-luminosity AGN is likely to be too low to account for much of the BELR in these objects), though which are the dominant models remains, to date, unknown.

In this paper we look at one aspect of activity in AGN connected with stars, and which is relevant to the work of Perry & Dyson (1985). We investigate the interaction of supernova ejecta with a hot, optically thin, QSO wind, in the presence of intense continuum radiation. In particular, we examine if shocked gas can radiate efficiently enough to cool to temperatures appropriate for the HIL.

The evolution of SNRs in a high-density static ambient medium has been previously studied by Terlevich et al. (1992), with particular application to the formation of BELRs in starburst models developed to obviate the existence of supermassive black holes in AGNs. Although there are similarities between this work and ours, a central difference is that these authors did not include Compton cooling or any heating processes in their calculations, and thus only considered the effect of a high ambient density on the SNR evolution. Our work also considers the influence of a powerful flux of ionizing radiation on the thermal evolution of the shocked regions.

2. DETAILS OF THE CALCULATIONS

Fits to the results of explosion models of type II supernovae indicate that power-law stratifications represent adequate approximations to ejecta density and velocity profiles (e.g., Woosley, Pinto, & Ensman 1988, and earlier work by Chevalier 1976 and Jones, Smith, & Straka 1981), and have been widely used in analytical and numerical studies of remnant evolution. If $\rho \propto r^{-n}$, these results indicate that $n \approx 12$ for the high-velocity ejecta.

Self-similar solutions for the structure of the shocked ejecta and swept-up medium for power-law density distributions in both of the unshocked components were derived by Chevalier (1982) and Nadyozhin (1985), following earlier work by Parker (1963). Their relevance to actual remnants was recently highlighted by high-resolution, spatially resolved VLBI observations of SN 1993J in M 81, which showed self-similar evolution of the azimuthally averaged radius (Marcaide et al. 1997). The observations are best fitted with $n \approx 12$, in good agreement with results from explosion models.

For $n \geq 3$, there must be an inner core of material with a shallower density profile ($\rho \propto r^{-\delta}$) in order for the mass of the ejecta to be finite. Such a core can be seen in the results of explosion models (e.g., Jones et al. 1981; Suzuki & Nomoto 1995). The solution is self-similar until the outer radius of the core reaches the position of the reverse shock, defined to occur at $t = t_{\rm dyn}$.

For our investigation we used the Chevalier-Nadyozhin similarity solution specified by $n = 12$, $\delta = 0$ as the initial profile for the SNR. While this is a simplification to actual distributions obtained from explosion models, it lends itself to the derivation of simple analytical expressions for the expected evolution (Pittard et al. 2001). In all our calculations we assumed a canonical explosion energy of 10^{51} ergs and ejecta mass of $10\,M_{\odot}$, which is typical of a SN of type II. Seventy five per cent of the mass and fifty eight per cent of the explosion energy are in the core. Figure 1 shows a typical density profile at $t = 0.1$ yr.

The hydrodynamics were evolved with an adaptive grid code which is second-order accurate in space and time (see e.g., Falle & Komissarov 1996, 1998), and which is ideally suited to this problem where regions which contain small-scale structure are located within much smoother regions.

Heating and cooling rates for a canonical AGN spectrum were kindly supplied by Tod Woods (cf. Woods et al. 1996) and are included in our calculation. They are tabulated as functions of temperature and ionization parameter, Ξ ($= F/cp$ where F is the local ionizing flux, c is the speed of light, and p is the gas pressure), and are valid in the optically thin, low-density regime. $\Xi = 2.3 P_{\rm rad}/P_{\rm gas}$ for fully ionized gas of cosmic abundance. The rates were calculated with the Cloudy photoionization code, its standard AGN spectrum, and Solar abundances. While abundances in AGN remain a very contentious issue,

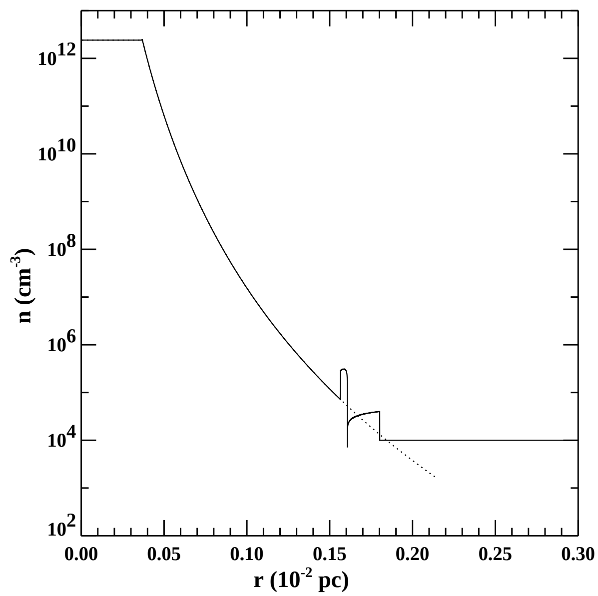

Fig. 1. The density profile for ejecta from a type II SN explosion, modeled as an $n = 12$ power law for the envelope and a $\delta = 0$ power law in the core, an explosion energy of 10^{51} erg, and an ejecta mass of $10\,M_\odot$. The dotted line shows the solution for ejecta expanding into a total vacuum. The solid line shows the case when the progenitor is surrounded by a constant density medium with $n = 10^4\,\mathrm{cm}^{-3}$: the outer part of the ejecta and the swept-up ambient medium are compressed into the Chevalier-Nadyozhin similarity form.

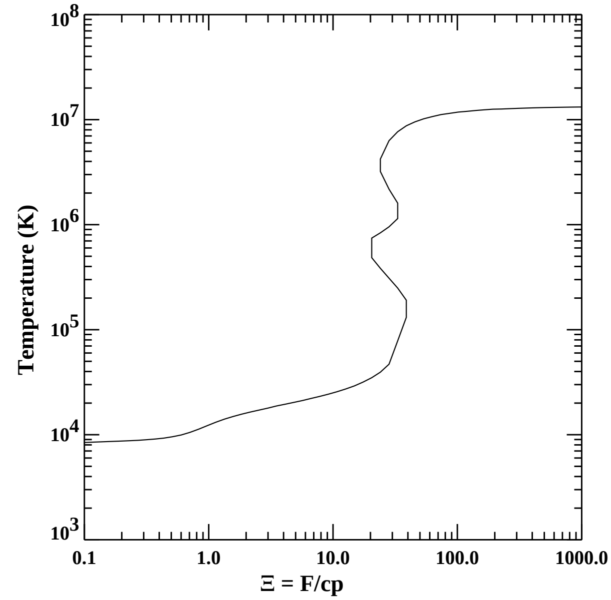

Fig. 2. Thermal equilibrium curve for the standard AGN spectrum in Cloudy (see Woods et al. 1996).

most theoretical work has been based on the assumption that the gas is of solar composition. Further details and assumptions can be found in Pittard et al. (2001) and Woods et al. (1996).

In Figure 2 we show the thermal equilibrium curve for the assumed AGN spectrum. At low temperatures, photoionization heating and cooling due to line excitation and recombination are in near balance. At high temperatures, the equilibrium arises from a balance of Compton heating and cooling. Note that the exact shape of the thermal equilibrium curve at intermediate temperatures is a complicated function of the irradiating spectrum, the assumed abundances and thermal processes (cf. Krolik, McKee, & Tarter 1981), and varies substantially from source to source. Since we are not modeling a specific object, we do not concern ourselves with the details of this part of the equilibrium curve.

To obtain cool gas in thermal equilibrium we require ionization parameters $\Xi \lesssim 10$. As noted by Perry & Dyson (1985), shocked gas cooled back to equilibrium can have a value of Ξ much lower than its pre-shock value. This is because Ξ does not change if the gas cools isobarically and the post-shock pressure is much greater than the pre-shock value. Therefore, strong shocks can create conditions for the gas to cool to temperatures much lower than the surrounding ambient temperature. The crucial question is whether the shocked gas remains at high pressures long enough to cool from its post-shock temperature to $T \sim 10^4$ K.

3. RESULTS

3.1. *1-D Models*

We start the evolution on the hydrodynamic grid at a time early enough for the dominant cooling of the shocked gas to be adiabatic expansion. As the remnant expands, radiative cooling gradually increases in importance, and a smooth transition from the adiabatic self-similar solution into the radiative regime occurs. As the remnant expands, the pre-shock ejecta are slowly heated from $T = 10^4$ K to $\sim 10^6$ K. We assume that the remnant is 0.33 pc distant from a central source with $L_{\rm ion} = 10^{47}\,\mathrm{erg\,s^{-1}}$, and is located in a region with a density $n = 10^6\,\mathrm{cm}^{-3}$.

In Figure 3 we show the evolution of the shocked region where divergence from the adiabatic self-similar solution is clearly seen. By $t = 1.0$ yr a region has formed with a temperature less than that of the undisturbed ambient medium. At $t = 1.4$ yr this region has a temperature of 7.0×10^5 K, and is coincident with a sharp growth in density. The profiles of ionization parameter show the gradual temporal increase in Ξ expected from the evolution of

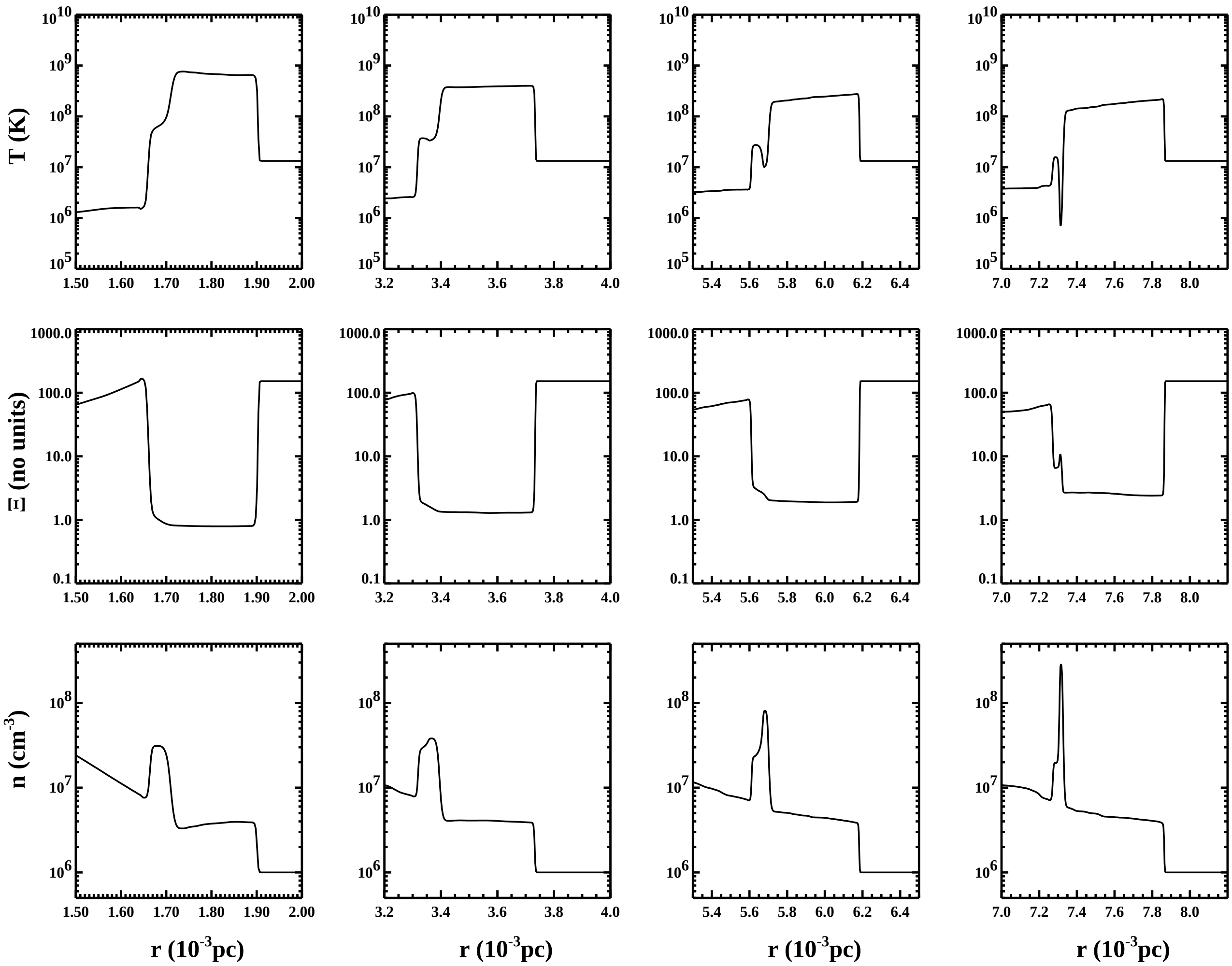

Fig. 3. The evolution of the remnant of a type II supernova for a constant density medium with $n = 10^6\,\mathrm{cm}^{-3}$ and $\Xi \approx 150$. The medium is stationary with respect to the remnant, and the entire area is immersed in a radiation field appropriate to an AGN of ionizing luminosity $10^{47}\,\mathrm{erg\,s}^{-1}$ with the central engine at a distance of 0.33 pc. The panels show from top to bottom the evolution of the temperature, the equilibrium ionization parameter, and the density of the region of hot shocked gas. This is bounded on its right edge by the forward shock propagating into the ambient medium and on its left edge by the reverse shock. From left to right the corresponding times are 0.2 yr, 0.5 yr, 1.0 yr, and 1.4 yr. The formation of a cooled region of gas can clearly be seen.

the self-similar solution. However, at $t = 1.4\,\mathrm{yr}$, the equilibrium ionization parameter associated with the cool material, Ξ_c, is substantially larger than that of the immediate surroundings, due to the cooling timescale becoming shorter than the dynamical timescale of the surrounding gas. At this point we stop our simulation, but note that Ξ_c will decrease on a sound-crossing timescale as the surrounding post-shock material gradually repressurizes the cool gas to its level. The density of the cool region, n_c, increases during this process, and in its final state the cool region is expected to have the following parameters: $\Xi_\mathrm{c} \approx 2$ to 3, $n_\mathrm{c} \approx \mathrm{few} \times 10^{10}\,\mathrm{cm}^{-3}$, $T_\mathrm{c} \lesssim 20{,}000\,\mathrm{K}$, and $N_\mathrm{H} \approx 10^{22}\,\mathrm{cm}^{-2}$. The radius of the remnant is $\approx 7.5 \times 10^{-3}\,\mathrm{pc}$ at this stage, while the expansion speed of the contact discontinuity (and thus the cool region) is $\approx 4 \times 10^8\,\mathrm{cm\,s}^{-1}$. Hence, our model results are in harmony with the temperature, ionization parameter, column density, and velocity dispersion of the observed HIL BELR clouds.

It is argued in Pittard et al. (2001) that since the shocked remnant gas rapidly depressurizes once the ejecta core interacts with the reverse shock (at $t = t_\mathrm{dyn}$), to form cool gas we require $t_\mathrm{cool} < t_\mathrm{dyn}$. In the above simulation this ratio is ≈ 0.4, and cool gas forms as expected. From simple expressions in Pittard et al. (2001) it can be shown that $t_\mathrm{cool}/t_\mathrm{dyn} \propto n^{-1/3}$, so we expect cool gas to form most easily

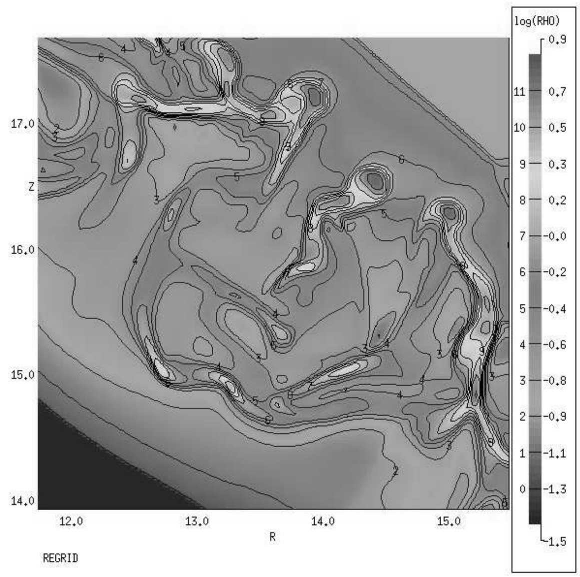

Fig. 4. The density structure contained within the shocked region of a SNR evolving into an ambient medium with density $n = 10^5\,\mathrm{cm}^{-3}$.

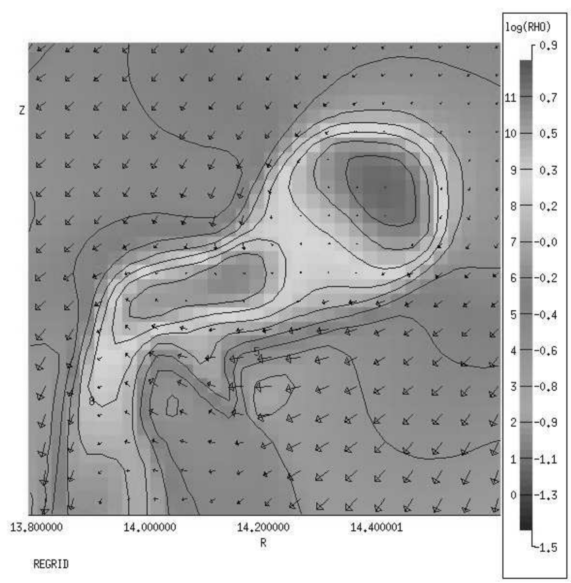

Fig. 5. The density structure of an individual cloud from within Figure 4. The flow field relative to the head of the cloud is also shown.

when the ambient density is high. An increased ambient density also yields a reduced value for Ξ at $t = t_{\rm cool}$. For an ambient density $n = 10^4$ cm^{-3}, $t_{\rm cool}/t_{\rm dyn} \approx 2$, and we do not expect cool gas to form in this case (cf. Pittard et al. 2001).

3.2. *2-D Models*

Extension of our models to 2-D axisymmetry allows us to investigate the effect of an external wind as opposed to a stationary medium, and here we present some preliminary results (Pittard et al. 2003).

In Figure 4 we show the edge of a remnant whose age is $t = 68\,\mathrm{yr}$ and which is expanding into stationary surroundings with $n = 10^5\,\mathrm{cm}^{-3}$. The forward shock is visible in the top right corner, and the reverse shock is visible in the bottom left corner. The initial interaction of the reverse shock with the ejecta core occurred at $t_{\rm dyn} \approx 15\,\mathrm{yr}$, and the shocked region is rapidly depressurizing. This figure shows the level of structure which we can expect in such simulations, although the details are likely to change in fully 3-D simulations. Of note is the fact that the cool regions (which we shall identify henceforth as 'clouds') form at the contact discontinuity between the shocked ejecta and the swept-up material, and contain within them a range of densities, equilibrium ionization parameters, and velocities.

Figure 5 shows a zoom onto an individual cloud from within Fig. 4. The head of the cloud is subsonic with respect to the surrounding flow, but the flow becomes mildly supersonic as it accelerates around the cloud. The cloud and most of the surroundings are continuing to cool at this stage, although some heating occurs in localized regions of low pressure and density. The clouds, being surrounded by a confining medium, are indeed long lived. Within an AGN as a whole, where many young SNRs will exist at a given time, there is a continual process of cloud creation and destruction. For an ambient medium with $n_e > 10^5\,\mathrm{cm}^{-3}$, the shocked gas cools more efficiently and the region of swept-up gas is thinner. In this case, the fact that the clouds have large momenta with respect to their surroundings causes them to move closer to the blast front than is seen in Fig. 4.

4. CONCLUSIONS

The results in § 3 demonstrate that it is possible to cool shocked supernova ejecta down to $T \sim 10^4\,\mathrm{K}$ in the inner regions of a QSO. Although our results differ from the original proposals of Dyson & Perry (1982) and Perry & Dyson (1985), which were for the shocked ambient medium to cool, the resulting cool gas nevertheless has properties (densities, column depths, velocities, and ionization parameters) compatible with those inferred for gas emitting the high-ionization lines in QSOs.

A parameter space study shows that for ambient densities of $n_e = 10^6$ to $10^7\,\mathrm{cm}^{-3}$, of order $2\,M_\odot$ of material can cool to low temperatures. Such gas then persists for $\sim 10\,\mathrm{yr}$ before the continuing expansion of the remnant reduces the density and pressure of the cool gas to the point where its equilibrium temperature and ionization parameter corresponds to the hot phase. This result is robust for a wide range of velocities of the ambient medium, although the spatial distribution of the cool gas around the limb of the remnant is sensitive to this detail.

A supernova rate of $1\,\mathrm{yr}^{-1}$ would imply a HIL mass of $\sim 20\,M_{\odot}$. This is easily compatible with the lower end of BELR mass estimates in the literature (e.g., Peterson 1997), although our model (and most others) would be severely challenged to explain much more extreme estimates of the mass of BELR gas (Baldwin et al. 2002 and references therein). It is currently unclear how this mass is partitioned between the HIL and LIL gas in these higher estimates.

Our investigation of the influence of a nuclear wind on the dynamics of the remnant is ongoing, and in the future we will also study the dynamical influence of the QSO radiation field. It is possible that a wind from a group of early-type stars may also provide the necessary conditions for the formation of cool regions, and this interaction may be more relevant in the nuclei of Seyfert galaxies, since supernova explosions will evacuate all but the most tightly bound gas (Perry & Dyson 1985). Finally, it is clear from our models that while the supernova-QSO wind interaction is conceptually simple, the BELR is likely to be a very complicated region in practice.

REFERENCES

Baldwin, J. A., Ferland, G. J., Korista, K. T., Hamann, F., & Dietrich, M. 2002, ApJ, in press (astro-ph/0209335)
Blandford, R. D., Netzer, H., Lodewijk, W., Courvoisier, T., & Mayor, M. 1990, Active Galactic Nuclei (Berlin: Springer)
Bottorff, M., Korista, K. T., Shlosman, I., & Blandford, R. D. 1997, ApJ, 479, 200
Cassidy, I., & Raine, D. J. 1996, A&A, 310, 49
Chevalier, R. A. 1976, ApJ, 207, 872
__________. 1982, ApJ, 258, 790
Clavel, J., et al. 1991, ApJ, 366, 64
Collin-Souffrin, S., Dumont, S., Joly, M., & Pequignot, D. 1986, A&A, 166, 27
Collin-Souffrin, S., Dumont, S., & Tully, J. 1982, A&A, 106, 362
Collin-Souffrin, S., Dyson, J. E., McDowell, J. C., & Perry, J. J. 1988, MNRAS, 232, 539
Dyson, J. E., & Perry, J. J. 1982, in Third European *IUE* Conference, eds. E. Rolfe, A. Heck, & B. Battrick (Noordwijk: ESA), 595
Emmering, R. T., Blandford, R. D., & Shlosman, I. 1992, ApJ, 385, 460
Falle, S. A. E. G., & Komissarov, S. S. 1996, MNRAS, 278, 586
__________. 1998, MNRAS, 297, 265
Ferland, G. J., Peterson, B. M., Horne, K., Welsh, W. F., & Nahar, S. N. 1992, ApJ, 387, 95
Fromerth, M. J., & Melia, F. 2001, ApJ, 549, 205
Gaskell, C. M. 1988, ApJ, 325, 114
Jones, E. M., Smith, B. W., & Straka, W. C. 1981, ApJ, 249, 185
Krolik, J. H., McKee, C. F., & Tarter, C. B. 1981, ApJ, 249, 422
Marcaide, J. M., et al. 1997, ApJ, 486, L31
Marziani, P., Sulentic, J. W., Dultzin-Hacyan, D., Calvani, M., & Moles, M. 1996, ApJS, 194, 37
Nadyozhin, D. K. 1985, Ap&SS, 112, 225
Parker, E. N. 1963, Interplanetary Dynamical Processes (New York: Interscience)
Perry, J. J., & Dyson, J. E. 1985, MNRAS, 213, 665
Peterson, B. M. 1997, An Introduction to Active Galactic Nuclei (Cambridge: Cambridge Univ. Press)
Pittard, J. M., Dyson, J. E., Falle, S. A. E. G., & Hartquist, T. W. 2001, A&A, 375, 827
Pittard, J. M., et al. 2003, in preparation
Roos, N. 1992, ApJ, 385, 108
Shields, J. C., Ferland, G. J., & Peterson, B. M. 1995, ApJ, 441, 507
Sulentic, J. W., Marziani, P., & Dultzin-Hacyan, D. 2000, ARA&A, 38, 521
Sulentic, J. W., Marziani, P., Dultzin-Hacyan, D., Calvani, M., & Moles, M. 1995, ApJ, 445, L85
Suzuki, T., & Nomoto, K. 1995, ApJ, 455, 658
Terlevich, R., Tenorio-Tagle, G., Franco, J., & Melnick, J. 1992, MNRAS, 255, 713
Williams, R. J. R, & Perry, J. J. 1994, MNRAS, 269, 538
Wills, B. J., Netzer, H., & Wills, D. 1985, ApJ, 288, 94
Woods, D. T., Klein, R. I., Castor, J. I., McKee, C. F., & Bell, J. B. 1996, ApJ, 461, 767
Woosley, S. E., Pinto, P. A., & Ensman, L. 1988, ApJ, 324, 466
Zurek, W. H., Siemiginowska, A., & Colgate, S. A. 1994, ApJ, 434, 46

John E. Dyson, Thomas W. Hartquist, and Julian M. Pittard: Department of Physics & Astronomy, The University of Leeds, Woodhouse Lane, Leeds, LS2 9JT, UK (jed,twh,jmp@ast.leeds.ac.uk).
Samuel A. E. G. Falle: Department of Applied Mathematics, The University of Leeds, Woodhouse Lane, Leeds, LS2 9JT, UK (sam@amsta.leeds.ac.uk).